Asian Journal of Control, Vol. 20, No. 4, pp. 1504–1518, July 2018
Published online 15 September 2017 in Wiley Online Library (wileyonlinelibrary.com) DOI: 10.1002/asjc.1640

CONTROL OF TWO ELECTRICAL PLANTS

José de Jesús Rubio, Jesus Lopez, Jaime Pacheco, and Rodrigo Encinas

ABSTRACT

In this paper, a controller is recommended for the regulation of two electrical plants. Since electrical plants generate electricity all the time, the regulation to get that all the plant states reach constant behaviors is important. Two main characteristics of the introduced method are: (i) it is based in the separation of the plant model equations, only some model equations are chosen for the regulation while the other model equations are ignored, it avoids the difficulty in the consideration of the full plant model; (ii) the Lyapunov strategy is employed to analyze the stability of the selected model equations in the electrical plant, it lets to ensure the regulation purpose. The advised method is applied in a gas turbine and a wind turbine for the electricity generation.

Key Words: Control, stability, electrical plant, gas turbine, wind turbine.

I. INTRODUCTION

Electricity generation is the technique of generating electric power from other sources of primary energy. For electric utilities, it is the first technique in the delivery of electricity to consumers. The other plants, electricity transmission, distribution, and electrical power storage and recovery using pumped-storage methods are normally carried out by the electric power industry. Electricity is most often generated at a power station by electromechanical generators, primarily driven by heat engines fuelled by combustion or nuclear fission but also by other means such as the kinetic energy of flowing water, gas, and wind. This research is focused in the electricity generation control by the gas fuel and wind energy.

There are some investigations about the control of gas turbines. In [1] and [2], mathematical models of the gas turbines are described. Optimal controls are addressed in [3] and [4]. In [5–7], feedback linearization techniques are employed. Strategies for power control are focused in [8] and [9]. In [10] and [11], proportional integral derivative controls are introduced. Several kinds of controls are proposed in [12–14]. In [15–17], adaptive controls are designed. The above discussed research shows that the control for the application in gas turbines is a novel topic.

There are some investigations about the control of wind turbines. Mathematical models of the wind turbines are presented in [18] and [19]. In [20–23], sliding mode controls are studied. Adaptive controls are investigated in [24,25]. In [26–28], robust controls are considered. H-infinity controls are suggested in [29,30]. Fault diagnosis methods are detailed in [31–33]. The aforementioned research shows that the control for the application in wind turbines is a current issue.

The states of the electrical plants of this study must be regulated, *i.e.*, all the states must reach constant references. This is due to the electrical plants generating electricity all the time. For this purpose, the next two issues must be taken into account:

1. The aforementioned investigations consider the regulation of the full plants, which is a problem due to the electrical plants of this study being underactuated, *i.e.* the number of states is bigger than the inputs number. It makes it difficult to reach the control purpose due to it is extreme difficulty in finding the gains of the controller which ensure the regulation. Consequently, another method for the regulation of this kind of plants must be designed.
2. Only some of the before mentioned works analyze the stability of their proposed controllers applied to the electrical plants, however, none has studied the uniform stability. The uniform stability is stronger than the stability due to the first is satisfied for any initial time, while the second is satisfied only for a zero initial time. Since, the stability of all the model equations lets to reach the regulation of the

Manuscript received March 9, 2017; revised June 17, 2017; accepted July 10, 2017.

The authors are with the Sección de Estudios de Posgrado e Investigación, Esime Azcapotzalco, Instituto Politécnico Nacional, Av. de las Granjas no. 682, Col. Santa Catarina, México D.F., 02250, México.

José de Jesús Rubio is the corresponding author (e-mail: jrubioa@ipn.mx; rubio.josedejesus@gmail.com).

The authors are grateful with the editor and with reviewers for their valuable comments and insightful suggestions, which can help to improve this research significantly. Authors thank the IPN, SIP, COFAA, and CONACYT for their help in this research.

© 2017 Chinese Automatic Control Society and John Wiley & Sons Australia, Ltd

electrical plant, the uniform stability of the electrical plant must be analyzed to ensure the regulation purpose.

This study advises a technique to solve the above mentioned issues which is detailed by the next two steps:

1. This investigation advises a method for the control of electrical plants which is based in the separation of the plant model equations, only some model equations are chosen for the regulation while the other model equations are ignored, it avoids the consideration of the full plant model which is more difficult. This method takes into account that the stability of all the model equations reach the regulation of the electrical plant. In the case that only the selected model equations of the electrical plant are chosen for the regulation, the non-selected model equations must have one of the next two characteristics to ensure the stability of all the model equations: (a) the non-selected model equations must be influenced by the selected model equations, in this way, the control of the non-selected model equations will be obtained by the control of the selected model equations; or (b) the non-selected model equations must be stable, in this way, the control of the selected model equations will be sufficient.
2. To ensure the regulation of the selected model equations in the electrical plant, the uniform stability of the closed loop model equations between the advised controller and the selected model equations is analyzed based on the Lyapunov technique. From the before point, the stability of the full electrical plant is gotten by ensuring the stability of the selected model equations. It is due to the not selected model equations are stable or are influenced by the selected model equations.

Finally, the suggested technique is applied to two electrical plants: gas and wind turbines. The gas turbine is applied for electricity generation from gas fuel. The wind turbine is applied for the electricity generation from wind energy.

These issues are discussed in the next sections. Section II introduces the recommended controller for the regulation of electrical plants. The suggested controller is applied for the regulation of a gas turbine in Section III. In Section IV, the mentioned controller is applied for the regulation of a wind turbine. Results of the control for the regulation of the gas and wind turbines are shown in the Section V. Section VI describes the conclusion and future research.

II. THE CONTROLLER OF THE ELECTRICAL PLANTS

In this section, the model is presented, the controller is recommended, and their stability is analyzed.

2.1 The electrical plant

In this subsection, the electrical plant is described. It has two main characteristics: (i) it is an underactuated plant, *i.e.*, it has more states than inputs; and (ii) it is a nonlinear plant, *i.e.*, it contains nonlinear functions such as exponential or potential.

Consider the next electrical plant:

$$\begin{aligned} \dot{Y} &= h(Y, W) \\ h(Y, W) &= \left[h_1(Y, W) \cdots h_L(Y, W) \right]^T \\ &\Rightarrow \dot{Y}_i = h_i(Y_i, W_i) \end{aligned} \tag{1}$$

where $Y = \left[y_1 \cdots y_L \right]^T \in \mathfrak{R}^L$ are states and $Y_i = \left[Y_1 \cdots Y_N \right]^T \in \mathfrak{R}^N$ are some grouped and selected states such that $Y_i \subset Y$, $L \gg N$, $W = \left[w_1 \cdots w_M \right]^T \in \mathfrak{R}^M$ are inputs and $W_i = \left[W_1 \cdots W_N \right]^T \in \mathfrak{R}^N$ are some grouped inputs such that $W_i \subseteq W$, $M \geq N$, $h(Y, W) \in \mathfrak{R}^L$ are continuous differentiable nonlinear functions and $h_i(Y_i, W_i) \in \mathfrak{R}^N$ are some selected and grouped nonlinear functions such that $h_i(Y_i, W_i) \subset h(Y, W)$. The underactuated characteristic of the plant satisfies $L \gg M \geq N$. The nonlinear characteristic of the plant is that it contains functions such as $e^{(\cdot)}$ or $(\cdot)^a$, where e is an exponential and a is a potency.

2.2 The suggested controller

In this subsection, controllers for the regulation of the selected model equations in the electrical plants are suggested. The objective of the controllers is that using the inputs, states of the selected model equations should reach constant behaviors, it is denoted as the regulation of the states by the controller.

Consider the next control functions:

$$W_i = -G_i Y_i \tag{2}$$

where $G_i \in \mathfrak{R}^{N \times N}$ are gains of the controllers.

Fig. 1 shows the suggested controllers where W_i are some selected inputs, Y_i are some selected states, and $h_i(\cdot)$ are some selected nonlinear functions.

Remark 1. The stability of all the model equations lets to reach the regulation of the electrical plant. In the case

© 2017 Chinese Automatic Control Society and John Wiley & Sons Australia, Ltd

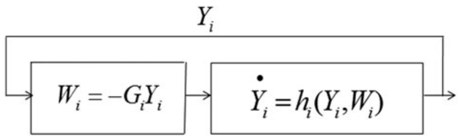

Fig. 1. The suggested controller.

that only the selected model equations of the electrical plant are chosen for the regulation as is described in (1), the not selected model equations must have one of the next two characteristics to ensure the stability of all the model equations: (a) the not selected model equations must be influenced by the selected model equations, in this way, the control of the not selected model equations will be gotten by the control of the selected model equations, or (b) the not selected model equations must be stable, in this way, the control of the selected model equations will be enough.

Remark 2. The drawback of the advised technique, is that if none of the two mentioned characteristics in the before remark is satisfied, the method of choosing only some model equations of the full electrical plant cannot be employed. In this case, the full electrical plant must be employed for the regulation and stability purposes.

2.3 The stability analysis

In this subsection, the stability of the advised controllers for the regulation of the electrical plants is analyzed. It is based in two parts, 1) the obtaining of the closed loop model equations, and 2) the stability analysis of the advised controllers.

First, the closed loop model equations of the recommended controllers applied for the regulation of the selected model equations will be gotten. It will be employed for the stability analysis.

Applying the Taylor series to (1) gives this result:

$$\dot{Y}_i = \frac{\partial h_i(Y_i, W_i)}{\partial Y_i}\left(Y_i - Y_{id}\right) + \frac{\partial h_i(Y_i, W_i)}{\partial W_i} \times \left(W_i - W_{id}\right) + R_i \tag{3}$$

where Y_{id} are desired states and W_{id} are desired inputs, Y_{id} and W_{id} are considered as zero due to it is the regulation case, R_i are residues. Adding and subtracting $\left\{ \frac{\partial h_i(Y_i,W_i)}{\partial Y_i}\Big|_{Y_i=0,W_i=0} \right\} Y_i$ and $\left\{ \frac{\partial h_i(Y_i,W_i)}{\partial W_i}\Big|_{Y_i=0,W_i=0} \right\} W_i$ to (3) gives:

$$\begin{aligned}
\dot{Y}_i &= \frac{\partial h_i(Y_i, W_i)}{\partial Y_i} Y_i + \frac{\partial h_i(Y_i, W_i)}{\partial W_i} W_i + R_i \\
&\quad + \left\{ \frac{\partial h_i(Y_i, W_i)}{\partial Y_i}\Big|_{Y_i=0,W_i=0} \right\} Y_i \\
&\quad - \left\{ \frac{\partial h_i(Y_i, W_i)}{\partial Y_i}\Big|_{Y_i=0,W_i=0} \right\} Y_i \\
&\quad + \left\{ \frac{\partial h_i(Y_i, W_i)}{\partial W_i}\Big|_{Y_i=0,W_i=0} \right\} W_i \\
&\quad - \left\{ \frac{\partial h_i(Y_i, W_i)}{\partial W_i}\Big|_{Y_i=0,W_i=0} \right\} W_i \\
\Rightarrow \dot{Y}_i &= \left\{ \frac{\partial h_i(Y_i, W_i)}{\partial Y_i}\Big|_{Y_i=0,W_i=0} \right\} Y_i \\
&\quad + \left\{ \frac{\partial h_i(Y_i, W_i)}{\partial W_i}\Big|_{Y_i=0,W_i=0} \right\} W_i \\
&\quad + \left[\frac{\partial h_i(Y_i, W_i)}{\partial Y_i} - \left\{ \frac{\partial h_i(Y_i, W_i)}{\partial Y_i}\Big|_{Y_i=0,W_i=0} \right\} \right] Y_i \\
&\quad + \left[\frac{\partial h_i(Y_i, W_i)}{\partial W_i} - \left\{ \frac{\partial h_i(Y_i, W_i)}{\partial W_i}\Big|_{Y_i=0,W_i=0} \right\} \right] W_i \\
&\quad + R_i
\end{aligned} \tag{4}$$

The equation (4) can be represented as:

$$\begin{aligned}
\dot{Y}_i &= A_i Y_i + B_i W_i + \tilde{A} Y_i + \widetilde{B} W_i + R_i \\
\Rightarrow \dot{Y}_i &= A Y_i + B W_i + \delta_i
\end{aligned} \tag{5}$$

where:

$$\begin{aligned}
A_i &= \left\{ \frac{\partial h_i(Y_i, W_i)}{\partial Y_i}\Big|_{Y_i=0,W_i=0} \right\} \\
B_i &= \left\{ \frac{\partial h_i(Y_i, W_i)}{\partial W_i}\Big|_{Y_i=0,W_i=0} \right\} \\
\tilde{A}_i &= \frac{\partial h_i(Y_i, W_i)}{\partial Y_i} - \left\{ \frac{\partial h_i(Y_i, W_i)}{\partial Y_i}\Big|_{Y_i=0,W_i=0} \right\} \\
\tilde{B}_i &= \frac{\partial h_i(Y_i, W_i)}{\partial W_i} - \left\{ \frac{\partial h_i(Y_i, W_i)}{\partial W_i}\Big|_{Y_i=0,W_i=0} \right\}
\end{aligned} \tag{6}$$

and $\delta_i = \tilde{A}_i Y_i + \tilde{B}_i W_i + R_i$ are unmodelled errors which are bounded such as $\left\|\delta_i\right\| \le \overline{\delta}_i$.

© 2017 Chinese Automatic Control Society and John Wiley & Sons Australia, Ltd

Substituting control functions (2) in the equation (5) produces:

$$\dot{Y}_i = A_i Y_i + B_i \left[-G_i Y_i\right] + \delta_i \Rightarrow \dot{Y}_i = A_{ci} Y_i + \delta_i \tag{7}$$

where $A_{ci} = A_i - B_i G_i$. The equation (7) are the closed loop model equations.

Second, the next Theorem is introduced to describe the stability analysis of the closed loop model equations.

Theorem 1. Consider controllers (2) for the regulation of the electrical plant (1). Let: A_i and B_i be described in (6) and A_{ci} be described in (7), λ_j be the eigenvalues of A_{ci}, and $Re\lambda_j$ be the real parts of the eigenvalues λ_j. Then 1.- The closed loop model equations (7) are uniformly stable if $Re\lambda_j < 0$ for all eigenvalues of A_{ci}. 2.- The closed loop model equations (7) are unstable if $Re\lambda_j > 0$ for one or more of the eigenvalues of A_{ci}.

Proof. Define the Lyapunov functions as:

$$V_i = Y_i^T P_i Y_i \tag{8}$$

Substituting closed loop model equations (7) in the derivatives of (8) produces:

$$\begin{aligned} \dot{V}_i &= \dot{Y}_i^T P_i Y_i + Y_i^T P \dot{Y}_i \\ &\Rightarrow \dot{V}_i = \left[A_{ci} Y_i + \delta_i\right]^T P_i Y_i + Y_i^T P_i \left[A_{ci} Y_i + \delta_i\right] \\ &\Rightarrow \dot{V}_i = Y_i^T \left[A_{ci}^T P_i + P_i A_{ci}\right] Y_i + 2 Y_i^T P_i \delta_i \end{aligned} \tag{9}$$

The last term satisfies the next inequality:

$$2 Y_i^T P_i \delta_i \leq \phi_i Y_i^T P_i Y_i + \frac{1}{\phi_i} \delta_i^T P_i \delta_i \tag{10}$$

where ϕ_i are small positive scalars. Substituting (10) into (9) gives:

$$\begin{aligned} \dot{V}_i &\leq Y_i^T \left[A_{ci}^T P_i + P_i A_{ci} + \phi_i P_i\right] Y_i + \frac{1}{\phi_i} \delta_i^T P_i \delta_i \\ &\Rightarrow \dot{V}_i \leq -Y_i^T Q_i Y_i + \frac{1}{\phi_i} \overline{\delta}_i^T P_i \overline{\delta}_i \end{aligned} \tag{11}$$

where equations $A_{ci}^T P_i + P_i A_{ci} + \phi_i P_i = -Q_i$ are satisfied with $P_i > 0$ and $Q_i > 0$ when $Re\lambda_j < 0$ for all eigenvalues of A_{ci}. Considering (8), the equation (11) can be rewritten as:

$$\begin{aligned} \dot{V}_i &\leq -Y_i^T Q_i P_i^{-1} P_i Y_i + \alpha_i \\ &\Rightarrow \dot{V}_i \leq -\lambda_{\min}(Q_i P_i^{-1}) Y_i^T P_i Y_i + \alpha_i \\ &\Rightarrow \dot{V}_i \leq -\gamma_i V_i + \alpha_i \end{aligned} \tag{12}$$

where $\alpha_i = \frac{1}{\phi_i} \overline{\delta}_i^T P_i \overline{\delta}_i$ and $\gamma_i = \lambda_{\min}(Q_i P_i^{-1})$. From (12) [11,15], and [17], it is proven that the closed loop model equations are uniformly stable. Then, the proof is determined.

Remark 3. Note that the above theorem does not say anything about the case when $Re\lambda_j \leq 0$ for all j, with $Re\lambda_j = 0$ for some j. In this case, the linearization fails to determine the stability.

III. THE CONTROL OF A GAS TURBINE

In this section, the controller of a gas turbine is studied. It is based in two parts, the mathematical model, and the controller design.

3.1 The mathematical model of the gas turbine

The gas turbine model consists of a compressor, a combustor, a compressor turbine, and a power turbine, as shown in the Figure 2 with its corresponding stage numbering. For the developed gas turbine model, component exit temperatures T_3, T_4, T_5, T_6, at different stages and the amount of mass stored in plenums M_3, M_4, M_5, M_6 are critical plant stages. The fuel flow rate m_f is the input of the plant.

3.1.1 The compressor

The compressor is represented by a volume-less component. The mathematical equation of the mass stored in the plenum m_3 in kg/s is:

$$\dot{m}_3 = MFDPm_{3cor} \left(\frac{P_2/P_{2ref}}{\left(T_2/T_{2ref}\right)^{0.5}} \right) - m_3 \tag{13}$$

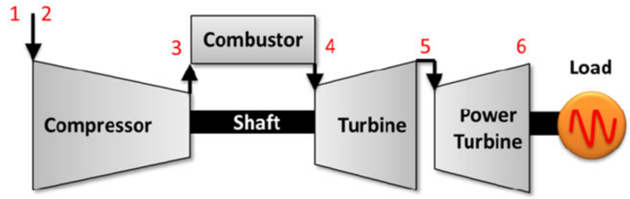

Fig. 2. Industrial gas turbine. [Color figure can be viewed at wileyonlinelibrary.com]

© 2017 Chinese Automatic Control Society and John Wiley & Sons Australia, Ltd

where T_2 is the input temperature in K, P_2 is the input pressure in Pa, the compressor temperature T_3 in K is:

$$\dot{T}_3 = \frac{1}{m_3 C_v}\left\{-m_3 R T_3 + \left[MFDPm_{3cor}\left(\frac{P_2/P_{2ref}}{\left(T_2/T_{2ref}\right)^{0.5}}\right) * \left(C_p T_2\left\{1+\frac{1}{\eta_c}\left[\left(\frac{P_3}{P_2}\right)^{\frac{\gamma-1}{\gamma}}-1\right]\right\} - C_v T_3\right)\right]\right\} \tag{14}$$

and the compressor pressure P_3 in Pa is:

$$P_3 = \frac{R}{V} m_3 T_3 \tag{15}$$

3.1.2 The combustor

The combustor is represented as a pure energy accumulator. The equation that describes burner dynamics in the combustor is:

$$\dot{T}_4 = \frac{(C_p - C_{vg}) m_a T_4 + (LHV\eta_b - C_{vg} T_4) m_f - m_g R T_4}{m_4 C_{vg}} - \sigma T_4 \tag{16}$$

where T_4 is the combustor temperature in K, m_f is the fuel flow rate and input. The mathematical equation of the mass stored in the plenum m_4 in kg/s is:

$$\dot{m}_4 = \left(m_3 + m_f\right) - m_4 \tag{17}$$

and the combustor pressure P_4 in Pa is:

$$P_4 = DPP_3 \tag{18}$$

3.1.3 The compressor turbine

In the compressor turbine, the mass stored in the plenum m_5 in kg/s is:

$$\dot{m}_5 = MFDPm_{5cor}\left(\frac{P_4/P_{4ref}}{\left(T_4/T_{4ref}\right)^{0.5}}\right) - m_5 \tag{19}$$

the temperature at the output of the compressor turbine T_5 in K is:

$$\dot{T}_5 = \frac{1}{m_5 C_v}\left\{-m_5 R T_5 + \left[MFDPm_{5cor}\left(\frac{P_4/P_{4ref}}{\left(T_4/T_{4ref}\right)^{0.5}}\right) * \left(C_p T_4\left\{1+\eta_t\left[1-\left(\frac{P_5}{P_4}\right)^{\frac{\gamma_g-1}{\gamma_g}}\right]\right\} - C_v T_5\right)\right]\right\} \tag{20}$$

and the compressor turbine pressure P_5 in Pa is:

$$P_5 = \frac{R}{V} m_5 T_5 \tag{21}$$

3.1.4 The power turbine

The power turbine component is represented in a similar way to the compressor turbine. The mathematical equation of the power turbine mass stored in the plenum m_6 in kg/s is:

$$\dot{m}_6 = MFDPm_{6cor}\left(\frac{P_5/P_{5ref}}{\left(T_5/T_{5ref}\right)^{0.5}}\right) - m_6 \tag{22}$$

the temperature at the output of the power turbine T_6 in K is:

© 2017 Chinese Automatic Control Society and John Wiley & Sons Australia, Ltd

$$\dot{T}_6 = \frac{1}{m_6 C_v}\left\{-m_6 R T_6 + \left[MFDPm_{6cor}\left(\frac{P_5/P_{5ref}}{\left(T_5/T_{5ref}\right)^{0.5}}\right)\right.\right.$$
$$\left.\left. * \left(C_p T_5\left\{1+\eta_{pt}\left[1-\left(\frac{P_6}{P_5}\right)^{\frac{\gamma_g-1}{\gamma_g}}\right]\right\} - C_v T_6\right)\right]\right\} \quad (23)$$

and the power turbine pressure P_6 in Pa is:

$$P_6 = \frac{R}{V} m_6 T_6 \quad (24)$$

$$\dot{y}_5 = \frac{1}{y_1 C_v}\left\{-y_1 R y_5 + \left[MFDPm_{3cor}\left(\frac{w_3/P_{2ref}}{\left(w_2/T_{2ref}\right)^{0.5}}\right) * \left(C_p w_2\left\{1+\frac{1}{\eta_c}\left[\left(\frac{y_9}{w_3}\right)^{\frac{\gamma-1}{\gamma}}-1\right]\right\} - C_v y_5\right)\right]\right\}$$

$$\dot{y}_6 = \frac{(C_p - C_{vg})m_a y_6 + (LHV\eta_b - C_{vg} y_6) w_1 - m_g R y_6}{y_2 Cvg} - \sigma y_6 \quad (26)$$

$$\dot{y}_7 = \frac{1}{y_3 C_v}\left\{-y_3 R y_7 + \left[MFDPm_{5cor}\left(\frac{y_{10}/P_{4ref}}{\left(y_6/T_{4ref}\right)^{0.5}}\right) * \left(C_p y_6\left\{1+\eta_t\left[1-\left(\frac{y_{11}}{y_{10}}\right)^{\frac{\gamma_g-1}{\gamma_g}}\right]\right\} - C_v y_7\right)\right]\right\}$$

$$\dot{y}_8 = \frac{1}{y_4 C_v}\left\{-y_4 R y_8 + \left[MFDPm_{6cor}\left(\frac{y_{11}/P_{5ref}}{\left(y_7/T_{5ref}\right)^{0.5}}\right) * \left(C_p y_7\left\{1+\eta_{pt}\left[1-\left(\frac{y_{12}}{y_{11}}\right)^{\frac{\gamma_g-1}{\gamma_g}}\right]\right\} - C_v y_8\right)\right]\right\}$$

3.1.5 The states space model

Inputs are defined as $w_1 = m_f$, $w_2 = T_2$, $w_3 = P_2$, states are $y_1 = m_3$, $y_2 = m_4$, $y_3 = m_5$, $y_4 = m_6$, $y_5 = T_3$, $y_6 = T_4$, $y_7 = T_5$, $y_8 = T_6$, $y_9 = P_3$, $y_{10} = P_4$, $y_{11} = P_5$, $y_{12} = P_6$. Mathematical equations for the masses stored in the plenum are:

$$\begin{aligned}
\dot{y}_1 &= MFDPm_{3cor}\left(\frac{w_3/P_{2ref}}{\left(w_2/T_{2ref}\right)^{0.5}}\right) - y_1 \\
\dot{y}_2 &= (y_1 + w_1) - y_2 \\
\dot{y}_3 &= MFDPm_{5cor}\left(\frac{y_{10}/P_{4ref}}{\left(y_6/T_{4ref}\right)^{0.5}}\right) - y_3 \\
\dot{y}_4 &= MFDPm_{6cor}\left(\frac{y_{11}/P_{5ref}}{\left(y_7/T_{5ref}\right)^{0.5}}\right) - y_4
\end{aligned} \quad (25)$$

Mathematical equations for the temperatures are:

Mathematical equations for the pressures are:

$$\begin{aligned}
y_9 &= \frac{R}{V} y_1 y_5 \\
y_{10} &= DP\frac{R}{V} y_1 y_5 \\
y_{11} &= \frac{R}{V} y_3 y_7 \\
y_{12} &= \frac{R}{V} y_4 y_8
\end{aligned} \quad (27)$$

© 2017 Chinese Automatic Control Society and John Wiley & Sons Australia, Ltd

Substituting the equation (40) into equations (38) and (39) gives the next states space model:

$$
\begin{aligned}
\dot{y}_1 &= MFDPm_{3cor}\left(\frac{w_3/P_{2ref}}{\left(w_2/T_{2ref}\right)^{0.5}}\right) - y_1\\
\dot{y}_2 &= \left(y_1 + w_1\right) - y_2\\
\dot{y}_3 &= MFDPm_{5cor}\left(\frac{\left(DP\frac{R}{V}y_1y_5\right)/P_{4ref}}{\left(y_6/T_{4ref}\right)^{0.5}}\right) - y_3\\
\dot{y}_4 &= MFDPm_{6cor}\left(\frac{\left(\frac{R}{V}y_3y_7\right)/P_{5ref}}{\left(y_7/T_{5ref}\right)^{0.5}}\right) - y_4\\
\dot{y}_5 &= \frac{1}{y_1C_v}\left\{-y_1Ry_5 + \left[MFDPm_{3cor}\left(\frac{w_3/P_{2ref}}{\left(w_2/T_{2ref}\right)^{0.5}}\right) * \left(C_pw_2\left\{1+\frac{1}{\eta_c}\left[\left(\frac{\frac{R}{V}y_1y_5}{w_3}\right)^{\frac{\gamma-1}{\gamma}} - 1\right]\right\} - C_vy_5\right)\right]\right\}\\
\dot{y}_6 &= \frac{(C_p - C_{vg})m_ay_6 + (LHV\eta_b - C_{vg}y_6)w_1 - m_gRy_6}{y_2Cvg} - \sigma y_6\\
\dot{y}_7 &= \frac{1}{y_3C_v}\left\{-y_3Ry_7 + \left[MFDPm_{5cor}\left(\frac{\left(DP\frac{R}{V}y_1y_5\right)/P_{4ref}}{\left(y_6/T_{4ref}\right)^{0.5}}\right) * \left(C_py_6\left\{1+\eta_t\left[1-\left(\frac{y_3y_7}{DPy_1y_5}\right)^{\frac{\gamma_g-1}{\gamma_g}}\right]\right\} - C_vy_7\right)\right]\right\}\\
\dot{y}_8 &= \frac{1}{y_4C_v}\left\{-y_4Ry_8 + \left[MFDPm_{6cor}\left(\frac{\left(\frac{R}{V}y_3y_7\right)/P_{5ref}}{\left(y_7/T_{5ref}\right)^{0.5}}\right) * \left(C_py_7\left\{1+\eta_{pt}\left[1-\left(\frac{y_4y_8}{y_3y_7}\right)^{\frac{\gamma_g-1}{\gamma_g}}\right]\right\} - C_vy_8\right)\right]\right\}
\end{aligned}
\tag{28}
$$

3.2 The controller of the gas turbine

In this subsection, the controller and stability are studied.

3.2.1 The control design

The objective of the controller is that using inputs, states of the gas turbine should reach constant behaviors, it is denoted as the regulation of the states. Some model equations are chosen from the electrical plant to be controlled, the first selected model equations of (41) are the combustor dynamics:

$$
\begin{aligned}
\dot{y}_1 &= MFDPm_{3cor}\left(\frac{w_3/P_{2ref}}{\left(w_2/T_{2ref}\right)^{0.5}}\right) - y_1\\
\dot{y}_5 &= \frac{1}{y_1C_v}\left\{-y_1Ry_5 + \left[MFDPm_{3cor}\left(\frac{w_3/P_{2ref}}{\left(w_2/T_{2ref}\right)^{0.5}}\right)\right.\right.\\
&\quad \left.\left. * \left(C_pw_2\left\{1+\frac{1}{\eta_c}\left[\left(\frac{\frac{R}{V}y_1y_5}{w_3}\right)^{\frac{\gamma-1}{\gamma}} - 1\right]\right\} - C_vy_5\right)\right]\right\}
\end{aligned}
\tag{29}
$$

© 2017 Chinese Automatic Control Society and John Wiley & Sons Australia, Ltd

and the second selected model equations of (41) are the compressor dynamics:

$$\dot{y}_2 = (y_1 + w_1) - y_2$$
$$\dot{y}_6 = \frac{(C_p - C_{vg})m_a y_6 + (LHV\eta_b - C_{vg}y_6)w_1 - m_g R y_6}{y_2 Cvg} - \sigma y_6 \tag{30}$$

From the equation (56), it can be observed that the control of the electrical plant for the first selected model equations is not complex because it has two inputs for the regulation of two states; therefore, the controller is:

$$\begin{aligned} w_2 &= -g_2 Y_2 \\ w_3 &= -g_3 Y_2 \end{aligned} \tag{31}$$

where $Y_2 = \begin{bmatrix} y_1 & y_5 \end{bmatrix}^T$ are states, w_2 and w_3 are control inputs, g_2 and g_3 are gains. From the equation (57), it can be observed that the controller for the second selected model equations is complex because it has one input for the regulation of two states; therefore, the controller is:

$$w_1 = -g_1 Y_1 \tag{32}$$

where $Y_1 = \begin{bmatrix} y_2 & y_6 \end{bmatrix}^T$ are states, w_1 is the control input, g_1 is the gain. Thus, the complete controller is:

$$\begin{aligned} w_1 &= -g_1 Y_1 \\ w_2 &= -g_2 Y_2 \\ w_3 &= -g_3 Y_2 \end{aligned} \tag{33}$$

3.2.2 Stability analysis

Making the linearization for the first selected model equations of the gas turbine model (56) gives the next result:

$$\dot{Y}_2 = A_2 Y_2 + B_2 W_2 \tag{34}$$

where:

$$A_2 = \begin{bmatrix} -1 & 0 \\ 0 & -\frac{R}{C_v} \end{bmatrix}$$
$$B_2 = \begin{bmatrix} 0 & 0 \\ 0 & 0 \end{bmatrix} \tag{35}$$

The control function (58) is:

$$W_2 = -G_2 Y_2 \tag{36}$$

where $G_2 = \begin{bmatrix} g_2 & g_3 \end{bmatrix}$, $W_2 = \begin{bmatrix} w_2 & w_3 \end{bmatrix}^T$. Substituting the control function in the linearized plant produces the next closed loop model equation:

$$\begin{aligned} \dot{Y}_2 &= A_2 Y_2 + B_2 \left[-G_2 Y_2\right] \\ \dot{Y}_2 &= \left[A_2 - B_2 G_2\right] Y_2 \\ \dot{Y}_2 &= A_{c2} Y_2 \end{aligned} \tag{37}$$

where $A_{c2} = A_2 - B_2 G_2$.

Making the linearization for the second selected model equations of the gas turbine model (56) yields:

$$\dot{Y}_1 = A_1 Y_1 + B_1 W_1 \tag{38}$$

where:

$$A_1 = \begin{bmatrix} -1 & 0 \\ 0 & -\sigma \end{bmatrix}$$
$$B_1 = \begin{bmatrix} 1 & 0 \end{bmatrix}^T \tag{39}$$

The control function (58) is:

$$W_1 = -G_1 Y_1 \tag{40}$$

where $G_1 = g_1$, $W_1 = w_1$. Substituting the control function in the linearized plant produces the next closed loop model equation:

$$\begin{aligned} \dot{Y}_1 &= A_1 Y_1 + B_1 \left[-G_1 Y_1\right] \\ \dot{Y}_1 &= \left[A_1 - B_1 G_1\right] Y_1 \\ \dot{Y}_1 &= A_{c1} Y_1 \end{aligned} \tag{41}$$

where $A_{c1} = A_1 - B_1 G_1$.

IV. THE CONTROL OF A WIND TURBINE

In this section, the controller of a wind turbine is studied. It is based in two parts, the mathematical model, and the controller design.

4.1 The mathematical model of the wind turbine

This subsection is divided in four parts, the first is the description of the mechanical model, the second is the description of the aerodynamic model, the third is

© 2017 Chinese Automatic Control Society and John Wiley & Sons Australia, Ltd

the description of the electrical model, and finally, the fourth is the combination of the aforementioned models to obtain the final mathematical model.

4.1.1 The mechanical model

Fig. 3 shows the wind turbine. A windward wind turbine of three blades with a rotatory tower is studied. The Euler Lagrangian method is employed to get this part of the model. Masses are concentrated at the center of mass. It can be seen that:

$$\begin{aligned} 3\left[J_1 + 1.5 m_2 l_{c2}^2\right]\ddot{\theta}_1 + 3b_{b1}\dot{\theta}_1 + 3k_{b1}\theta_1 &= \tau_1 \\ 3\left[J_2 + m_2 l_{c2}^2\right]\ddot{\theta}_2 + 3b_{b2}\dot{\theta}_2 + 3k_{b2}\theta_2 + 2\pi k_{b2} &= \tau_2 \end{aligned} \tag{42}$$

where $\tau_1 = \tau_{1a} + \tau_{1b} + \tau_{1c}$ and $\tau_2 = \tau_{2a} + \tau_{2b} + \tau_{2c}$. τ_2 of (42) is:

$$\begin{aligned} \tau_2 &= C_1 F_2 \\ F_2 &= F_{2a} + F_{2b} + F_{2c} \end{aligned} \tag{43}$$

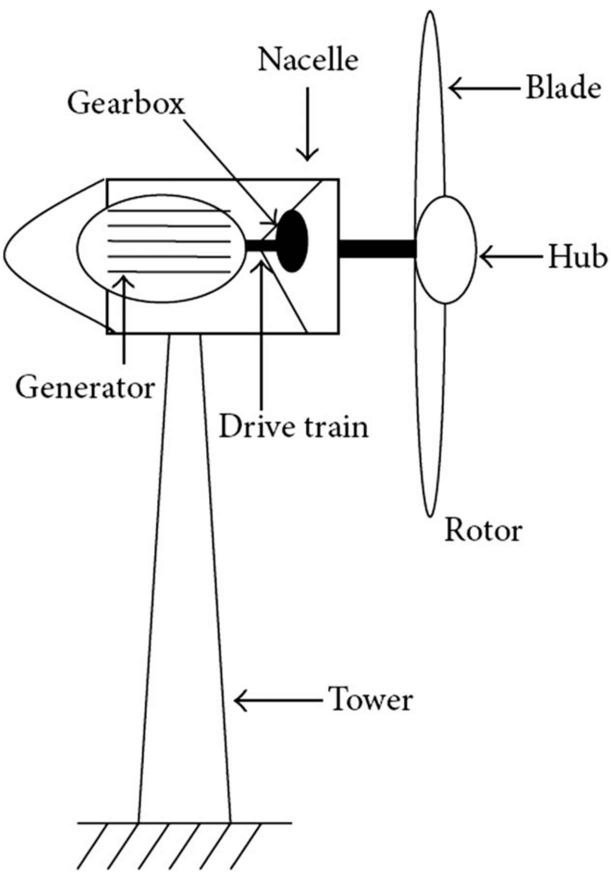

Fig. 3. Wind turbine.

where $C_1 = \cos(\theta_1)$, F_{2a}, F_{2b} and F_{2c} are the force of air received by three blades. The equation (43) describes the assumption that the air goes in one direction, if $\theta_1 = 0$, then the maximum air intake moves blades of the wind turbine, but if the tower turns to the left or to the right and θ_1 changes, then the wind turbine turns, and the air intake decreases. τ_1 of (42) is:

$$\tau_1 = k_m i_1 \tag{44}$$

where k_m is a motor magnetic flux constant of the tower, and i_1 is the motor current of the tower in A. Equations (42), (43), and (44) are the main equations of the mechanical model that represents the turbine and tower.

4.1.2 The aerodynamic model

The aerodynamic model is the mathematical model of the torque applied to the blades. The mechanical power captured by the turbine P_a is:

$$P_a = F_{2a}\dot{\theta}_2 = \frac{1}{2}\rho A C_p(\lambda, \beta) V_\omega^3 \tag{45}$$

where ρ is the air density, $A = \pi R^2$ is the area swept by rotor blades with radius R, V_ω is the wind speed, $C_p(\lambda, \beta)$ is the performance coefficient of the wind turbine, whose value is a function of the tip speed ratio λ, is:

$$\lambda = \frac{\dot{\theta}_2 R}{V_\omega} \tag{46}$$

For the purpose of simulation, the model of $C_p(\lambda, \beta)$ is:

$$C_p(\lambda, \beta) = c_1\left(\frac{c_2}{\lambda_j} - c_3\beta - c_4\right)e^{-c_5/\lambda_j} + c_6\lambda \tag{47}$$

where:

$$\frac{1}{\lambda_j} = \frac{1}{\lambda + 0.08\beta} - \frac{0.035}{\beta^3 + 1} \tag{48}$$

and coefficients are $c_1 = 0.5176$, $c_2 = 116$, $c_3 = 0.4$, $c_4 = 5$, $c_5 = 21$, $c_6 = 0.0068$, and β is the blade pitch angle. Using equations (43), (45), (46), (47), and (48) produces the next mathematical model of the torque applied to wind turbine blades:

© 2017 Chinese Automatic Control Society and John Wiley & Sons Australia, Ltd

$$
\begin{aligned}
\tau_2 &= C_1\left(F_{2a}+F_{2b}+F_{2c}\right)\\
F_{2a} &= \frac{1}{2\dot{\theta}_2}\rho A C_p(\lambda,\beta)V_\omega^3\\
F_{2b} &= \frac{1}{2\dot{\theta}_2}\rho A C_p(\lambda,\beta)V_\omega^3\\
F_{2c} &= \frac{1}{2\dot{\theta}_2}\rho A C_p(\lambda,\beta)V_\omega^3
\end{aligned} \tag{49}
$$

where C_1 is explained in (43), λ is explained in (46), $C_p(\lambda,\beta)$ is explained in (47), and λ_j is explained in (48).

4.1.3 The electrical model

Mathematical models of the motor and generator are:

$$
\begin{aligned}
V_1 &= R_1 i_1 + L_1 \dot{i}_1 + k_1\dot{\theta}_1\\
k_2\dot{\theta}_2 &= R_2 i_2 + L_2 \dot{i}_2 + V_2
\end{aligned} \tag{50}
$$

where k_1 and k_2 are the motor and generator back emf constants, R_1 and R_2 are the motor and generator resistances, L_1 and L_2 are the motor and generator inductances, V_1 and V_2 are the motor and generator voltages in V, i_1 and i_2 are the motor and generator currents in A. For the generator of this research $V_2 = R_e i_2$. Thus, (50) is:

$$
\begin{aligned}
V_1 &= R_1 i_1 + L_1 \dot{i}_1 + k_1\dot{\theta}_1\\
k_2\dot{\theta}_2 &= \left(R_2+R_e\right) i_2 + L_2 \dot{i}_2\\
V_2 &= R_e i_2
\end{aligned} \tag{51}
$$

4.1.4 The states space model

Define state variables as $y_1 = i_2$, $y_2 = \theta_2$, $y_3 = \dot{\theta}_2$, $y_4 = i_1$, $y_5 = \theta_1$, $y_6 = \dot{\theta}_1$, inputs as $w_1 = F_2$, $w_2 = V_1$. Consequently, the mathematical model of the equations (42), (44), (46), (49), and (51) is:

$$
\begin{aligned}
\dot{y}_1 &= -\frac{\left(R_2+R_e\right)}{L_2}y_1 + \frac{k_2}{L_2}y_3\\
\dot{y}_2 &= y_3\\
\dot{y}_3 &= -\frac{k_{b2}}{\left[J_2+m_2 l_{c2}^2\right]}y_2 - \frac{b_{b2}}{\left[J_2+m_2 l_{c2}^2\right]}y_3\\
&\quad - \frac{2\pi k_{b2}}{3\left[J_2+m_2 l_{c2}^2\right]} + \frac{\cos(y_5)}{3\left[J_2+m_2 l_{c2}^2\right]}w_1\\
\dot{y}_4 &= -\frac{R_1}{L_1}y_4 - \frac{k_1}{L_1}y_6 + \frac{1}{L_1}w_2\\
\dot{y}_5 &= y_6\\
\dot{y}_6 &= -\frac{k_{b1}}{\left[J_1+1.5 m_2 l_{c2}^2\right]}y_5\\
&\quad - \frac{b_{b1}}{\left[J_1+1.5 m_2 l_{c2}^2\right]}y_6\\
&\quad + \frac{k_m}{3\left[J_1+1.5 m_2 l_{c2}^2\right]}y_4\\
w_1 &= F_{2a}+F_{2b}+F_{2c}\\
F_{2a} &= F_{2b} = F_{2c} = \frac{1}{2y_3}\rho A C_p(\lambda,\beta)V_\omega^3\\
C_p(\lambda,\beta) &= c_1\left(\frac{c_2}{\lambda_j} - c_3\beta - c_4\right)e^{-c_5/\lambda_j} + c_6\lambda\\
\lambda &= \frac{y_3 R}{V_\omega},\quad \frac{1}{\lambda_j} = \frac{1}{\lambda+0.08\beta} - \frac{0.035}{\beta^3+1}
\end{aligned} \tag{52}
$$

4.2 The controller of the wind turbine

In this subsection, the controller and stability are studied.

4.2.1 The controller design

The objective of the controller is that using the input, states of the wind turbine should reach constant behaviors, it is known as the regulation of the states.

In this case, the full electrical plant is employed for the regulation; consequently, the electrical plant of (52) is:

© 2017 Chinese Automatic Control Society and John Wiley & Sons Australia, Ltd

$$\begin{aligned}
\dot{y}_1 &= -\frac{\left(R_2 + R_e\right)}{L_2} y_1 + \frac{k_2}{L_2} y_3 \\
\dot{y}_2 &= y_3 \\
\dot{y}_3 &= -\frac{k_{b2}}{\left[J_2 + m_2 l_{c2}^2\right]} y_2 - \frac{b_{b2}}{\left[J_2 + m_2 l_{c2}^2\right]} y_3 \\
&\quad - \frac{2\pi k_{b2}}{3\left[J_2 + m_2 l_{c2}^2\right]} + \frac{\cos(y_5)}{3\left[J_2 + m_2 l_{c2}^2\right]} w_1 \\
\dot{y}_4 &= -\frac{R_1}{L_1} y_4 - \frac{k_1}{L_1} y_6 + \frac{1}{L_1} w_2 \\
\dot{y}_5 &= y_6 \\
\dot{y}_6 &= -\frac{k_{b1}}{\left[J_1 + 1.5 m_2 l_{c2}^2\right]} y_5 - \frac{b_{b1}}{\left[J_1 + 1.5 m_2 l_{c2}^2\right]} y_6 \\
&\quad + \frac{k_m}{3\left[J_1 + 1.5 m_2 l_{c2}^2\right]} y_4
\end{aligned} \tag{53}$$

From the equation (53), it can be seen that the control of the plant is complex because it has 1 input for the regulation of 6 states; therefore, the controller is:

$$\begin{aligned} w = w_2 &= -gY \\ w_1 &= 0 \end{aligned} \tag{54}$$

where $Y = \left[y_1\ y_2\ y_3\ y_4\ y_5\ y_6\right]^T$ are states, w is the control input, g is the gain.

4.2.2 The stability analysis

Making the linearization of the wind turbine model (53) produces the next result:

$$\dot{Y} = AY + BW \tag{55}$$

where:

$$A = \begin{bmatrix} a_{11} & 0 & a_{13} & 0 & 0 & 0 \\ 0 & 0 & 1 & 0 & 0 & 0 \\ 0 & a_{32} & a_{33} & 0 & 0 & 0 \\ 0 & 0 & 0 & a_{44} & 0 & a_{46} \\ 0 & 0 & 0 & 0 & 0 & 1 \\ 0 & 0 & 0 & a_{64} & a_{65} & a_{66} \end{bmatrix}$$
$$B = \left[0\ 0\ 0\ \tfrac{1}{L_1}\ 0\ 0\right]^T \tag{56}$$

where $a_{11} = -\frac{(R_2+R_e)}{L_2}$, $a_{13} = \frac{k_2}{L_2}$, $a_{32} = -\frac{k_{b2}}{\left[J_2+m_2 l_{c2}^2\right]}$, $a_{33} = -\frac{b_{b2}}{\left[J_2+m_2 l_{c2}^2\right]}$, $a_{44} = -\frac{R_1}{L_1}$, $a_{46} = -\frac{k_1}{L_1}$, $a_{64} = \frac{k_m}{3\left[J_1+1.5 m_2 l_{c2}^2\right]}$, $a_{65} = -\frac{k_{b1}}{\left[J_1+1.5 m_2 l_{c2}^2\right]}$, $a_{66} = -\frac{b_{b1}}{\left[J_1+1.5 m_2 l_{c2}^2\right]}$.

The control function (58) is:

$$W = -GY \tag{57}$$

where $G = g$, $W = w$. Substituting the control function produces next closed loop model equation:

$$\begin{aligned} \dot{Y} &= AY + B\left[-GY\right] \\ \dot{Y} &= \left[A - BG\right] Y \\ \dot{Y} &= A_c Y \end{aligned} \tag{58}$$

where $A_c = A - BG$.

V. RESULTS

In this section, the suggested controller called SC will be compared with the sliding mode controller of [20–23] called SMC for states regulation of two electrical plants which are the gas and wind turbines. The objective is that states of the plant y should reach constant behaviors, it is understood as a good regulation of the states. The sliding mode controller of [20–23] is selected for the comparisons because it is applied to a wind turbine. In the next two subsections, the root mean square error (RMSE) will be used in the comparisons, it is:

$$ECM = \left(\frac{1}{T}\int_0^T y^2 d\tau\right)^{\frac{1}{2}} \tag{59}$$

where $y^2 = y_1^2 + y_5^2$ for the first selected model equations and $y^2 = y_2^2 + y_6^2$ for the second selected model equations in the gas turbine, and $y^2 = y_1^2 + y_1^2 + y_3^2 + y_4^2 + y_5^2 + y_6^2$ for the wind turbine, and T is the final time.

5.1 Gas turbine

Table I shows parameter values for the gas turbine.

The SMC of [20–23] is employed where initial conditions are $y_{s0} = [76, 76, 76, 76, 691.7694, 1616.4, 1270.8, 932.4205]^T$, and gains are $g_{s1} = [-4.2, -5.6]$, $g_{s2} = [-2 \times 10^{-3}, -1 \times 10^{-3}]$, $g_{s3} = [-1 \times 10^{-3}, -1 \times 10^{-3}]$.

The SC of the equation (33) is utilized where initial conditions are $y_0 = [76, 76, 76, 76, 691.7694, 1616.4, 1270.8, 932.4205]^T$, and gains are $g_1 = [4.2 \times 10^2, -5.6 \times 10^1]$, $g_2 = [2, 1]$, $g_3 = [10, 10]$. Substituting values of Table I and values of the gains in the matrix A_{c2} of (37), the next result is obtained:

$$A_{c2} = \begin{bmatrix} -1.0 & 0.0 \\ 0.0 & -0.39972 \end{bmatrix} \tag{60}$$

© 2017 Chinese Automatic Control Society and John Wiley & Sons Australia, Ltd

Table I. Parameter values for the gas turbine

Parameter	Value	Parameter	Value
$MFDP$ [kg/s]	1×10^{-2}	P_{2ref} [Pa]	103.125
m_{3cor} [kg/s]	7.731	T_{2ref} [K]	288.15
C_p [(J/kg)K]	1005	η_c [-]	1.46966
C_v [(J/kg)K]	718	V [m^3]	0.8
R [(J/kg)K]	287	η_b [-]	0.99
LHV [(J/kg)K]	44124	η_t [-]	1×10^{-4}
m_a [kg/s]	76	DP [Pa]	0.99
m_g [kg/s]	32.94229	η_{pt} [-]	1×10^{-4}
P_{4ref} [Pa]	680.125	T_{4ref} [K]	1400
C_{vg} [(J/kg)K]	863	γ [-]	1.4
P_{5ref} [Pa]	416.0	T_{5ref} [K]	1000
m_{5cor} [kg/s]	2.7184	σ [-]	1×10^{-6}
m_{6cor} [kg/s]	0.3912	γ_g [-]	1.33

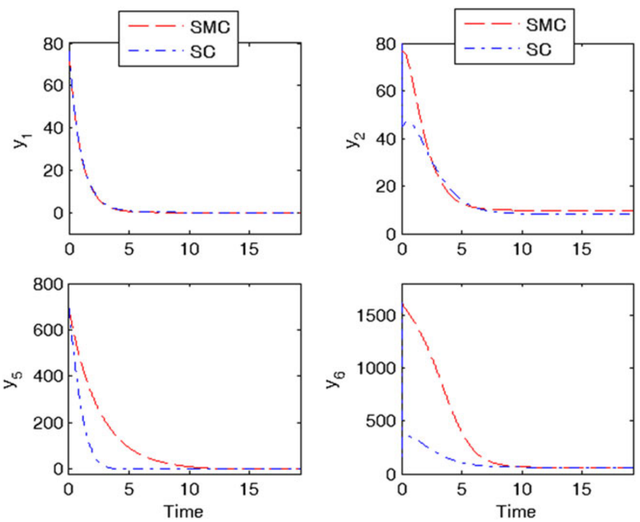

Fig. 4. Combustor and compressor states. [Color figure can be viewed at wileyonlinelibrary.com]

Eigenvalues are $\lambda_1 = -0.39973$, $\lambda_2 = -0.99997$. Therefore, the first selected model equations of the electrical plant are uniformly stable. Substituting values of Table I and values of the gains in the Matrix A_{C1} of (41) produces the next result:

$$A_{c1} = \begin{bmatrix} -421.0 & 56.0 \\ 0.0 & -1.0\times10^{-6} \end{bmatrix} \tag{61}$$

Eigenvalues are $\lambda_1 = -1.0\times10^{-6}$, $\lambda_2 = -421.00$. Therefore, the second selected model equations of the electrical plant are uniformly stable.

Figs 4 and 5 show combustor and compressor states, and turbines states of the gas turbine with controllers for a time from 0 s to 19.2 s. Table II shows the RMSE of (59)

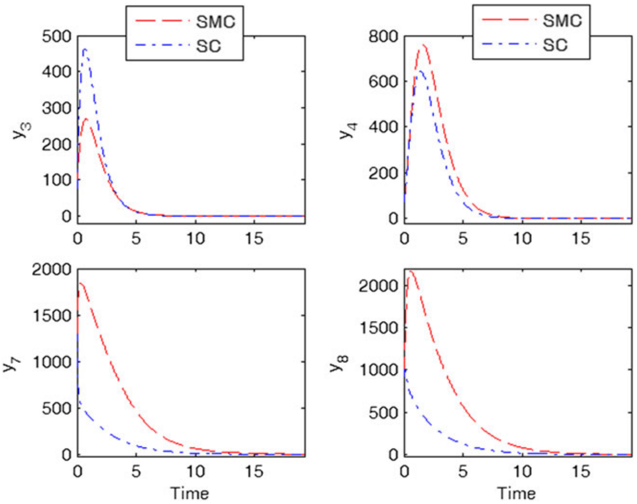

Fig. 5. Turbines states. [Color figure can be viewed at wileyonlinelibrary.com]

Table II. Results for the gas turbine

Methods	RMSE-FSME	RMSE-SSME
SMC	125.2273	411.4160
SC	82.1330	100.2606

where RMSE-FSME is the RMSE for the first selected model equations and RMSE-SSME is the RMSE for the second selected model equations.

Note that the turbines behaviors are influenced by the combustor and compressor behaviors; therefore, regulation of the second is the objective because it produces the regulation of the first. From Figs 4 and 5, it can be seen that SC reaches a better regulation than SMC because the plant signals for the first reaches better the constant behaviors than for the second. From Table II, it can be seen that SC reaches better accuracy than SMC because the RMSE for the first is smaller than for the second. Thus, SC is preferable for the states regulation in a gas turbine.

5.2 Wind turbine

Table III shows parameter values for the wind turbine.

The SMC of [20–23] is employed where initial conditions are $y_{s0} = [0.1, 0.1, 0.1, 0.1, 0.1, 0.1]^T$, and the gain is $g_s = [0, 0, -1\times10^{-3}, 0, 0, 0]$.

The SC of the equation (33) is utilized where initial conditions are $y_0 = [0.1, 0.1, 0.1, 0.1, 0.1, 0.1]^T$, and the gain is $g_1 = [0, 0, -1\times10^{-3}, 0, 0, 0]$. Substituting values of Table III and the value of the gain in the Matrix A_C of (58) the next result is obtained:

© 2017 Chinese Automatic Control Society and John Wiley & Sons Australia, Ltd

Table III. Parameter values for the wind turbine

Parameter	Value	Parameter	Value
k_{b1} [kgm^2/s^2]	1×10^{-6}	R_e [Ω]	30
b_{b1} [kgm^{2}rad/s]	0.1	k_m [Wb]	0.09
k_{b2} [kgm^2/s^2]	1×10^{-6}	l_{c2} [m]	0.5
b_{b2} [kgm^{2}rad/s]	0.1	m_2 [kg]	0.5
k_2 [Vs/rad]	0.45	R [m]	0.5
$J_1 = J_2$ [kgm^2]	0.01273	R_1 [Ω]	18
L_2 [H]	0.6031	g [m/s^2]	9.81
k_1 [Vs/rad]	0.0045	V_ω [m/s]	5
ρ [kg/m^3]	1.225	β [rad]	0.5
L_1 [H]	0.6031	R_2 [Ω]	6.96

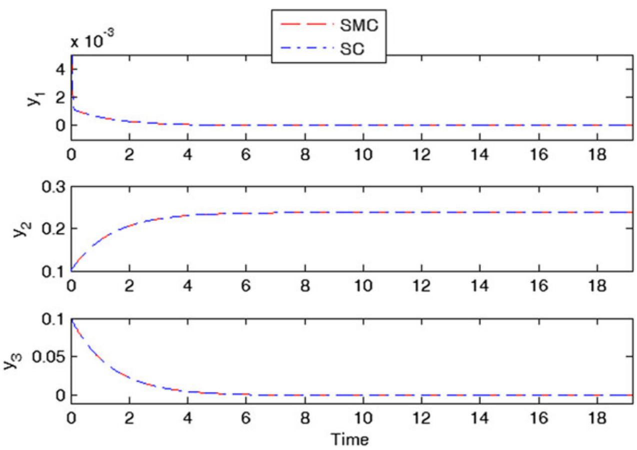

Fig. 6. Turbine states. [Color figure can be viewed at wileyonlinelibrary.com]

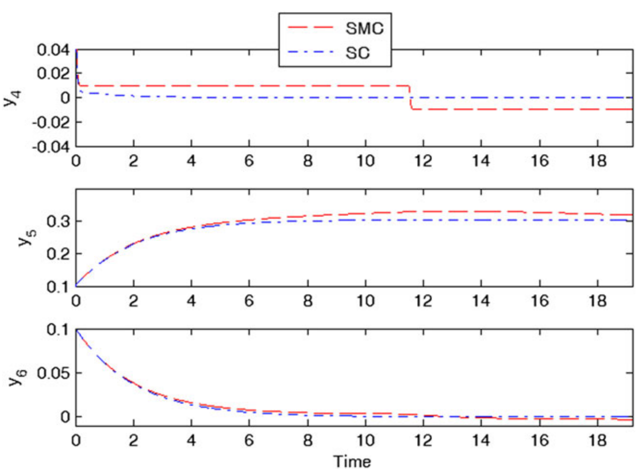

Fig. 7. Tower states. [Color figure can be viewed at wileyonlinelibrary.com]

Table IV. Results for the wind turbine

Methods	RMSE
SMC	0.2686
SC	0.2594

$$A_c = \begin{bmatrix} a_{c11} & 0 & a_{c13} & 0 & 0 & 0 \\ 0 & 0 & 1 & 0 & 0 & 0 \\ 0 & a_{c32} & a_{c33} & 0 & 0 & 0 \\ 0 & 0 & a_{c43} & a_{c44} & 0 & a_{c46} \\ 0 & 0 & 0 & 0 & 0 & 1 \\ 0 & 0 & 0 & a_{c64} & a_{c65} & a_{c66} \end{bmatrix} \quad (62)$$

where $a_{c11} = -61.283$, $a_{c13} = 0.74614$, $a_{c32} = -7.2606 \times 10^{-6}$, $a_{c33} = -0.72606$, $a_{c43} = 1.6581 \times 10^{-3}$, $a_{c44} = -29.846$, $a_{c46} = -7.4614 \times 10^{-3}$, $a_{c64} = 0.14983$, $a_{c65} = -4.9943 \times 10^{-6}$, $a_{c66} = -0.49943$. Eigenvalues are $\lambda_1 = -9.9995 \times 10^{-6} + 7.4944 \times 10^{-8}i$, $\lambda_2 = -9.9995 \times 10^{-6} - 7.4944 \times 10^{-8}i$, $\lambda_3 = -0.49947$, $\lambda_4 = -61.282$, $\lambda_5 = -29.847$, $\lambda_6 = -0.72603$. Therefore, the full electrical plant is uniformly stable.

Figs 6 and 7 show the turbine states and tower states of the wind turbine with controllers for a time from 0 s to 19.2 s. Table IV shows the RMSE of (59).

Note that the regulation objective is complex because there is only one input for the regulation of six states; nevertheless, the main objective is reached due to all the states in the wind turbine are regulated with the advised controller. From Figs 6 and 7, it can be seen that the SC reaches a better regulation than SMC because the plant signals for the first reaches better the constant behaviors than for the second. From Table IV, it can be seen that SC reaches better accuracy than SMC because the RMSE for the first is smaller than for the second. Thus, SC is preferable for the states regulation in a wind turbine.

VI. CONCLUSIONS

In this research, a controller is advised for the regulation of states in two electrical plants. The main issue is that the control of the electrical plants of this study is difficult due to they are underactuated, *i.e.* there are more states than inputs; consequently, an alternative solution of this issue is suggested in this paper. The advised controller is compared with the sliding mode controller for the states regulation in a gas turbine and a wind turbine producing that the first achieved better accuracy in comparison with the second due to in the first all the states reach the constant behaviors faster that in the

© 2017 Chinese Automatic Control Society and John Wiley & Sons Australia, Ltd

second. The recommended controller could be applied to other kind of electrical, mechanical, hydraulic, pneumatic, robotic, or mechatronic plants. In the future, other kind of controllers will be designed for the regulation, for the trajectory tracking, for the disturbance rejection in the two electrical plants, or the intelligent algorithms will be used for the behavior learning in the electrical plants [34,35].

REFERENCES

1. Tsoutsanis, E., N. Meskin, M. Benammar, and K. Khorasani, "A component map tuning method for performance prediction and diagnostics of gas turbine compressors," *Appl. Energy*, Vol. 135, pp. 572–585 (2014).
2. Rahme, S. and N. Meskin, "Adaptive sliding mode observer for sensor fault diagnosis of an industrial gas turbine," *Control Eng. Practice*, Vol. 38, pp. 57–74 (2015).
3. Alhajaja, A., N. M. Dowellb, and N. Shah, "A techno-economic analysis of post-combustion co_2 capture and compression applied to a combined cycle gas turbine: part II. Identifying the cost-optimal control and design variables," *Int. J. Greenh. Gas Control*, Vol. 52, pp. 331–343 (2016).
4. Wu, W., S. A. Chen, J. J. Hwang, and F. T. Hsu, "Optimization and control of a stand-alone hybrid solid oxide fuel cells/gas turbine system coupled with dry reforming of methane," *J. Process Control*, Vol. 54, pp. 90–100 (2017).
5. Bonfiglio, A., S. Cacciacarne, M. Invernizzi, R. Procopio, S. Schiano, and I. Torre, "Gas turbine generating units control via feedback linearization approach," *Energy*, Vol. 121, pp. 491–512 (2017).
6. Li, Y., J. Lu, X. Mao, and Q. Qiu, "Stabilization of hybrid systems by feedback control based on discrete-time state and mode observations," *Asian J. Control*, Vol. 20, No. 1, pp. 1–11 (2018).
7. Zhen, Z., S. X. Tang, and Z. Zhou, "Stabilization of a heat-ode system cascaded at a boundary point and an intermediate point," *Asian J. Control*, Vol. 19, No. 6, pp. 1–10 (2017).
8. Duan, J., S. Fan, F. Wu, L. Sun, and G. Wang, "Power balance control of micro gas turbine generation system based on super capacitor energy storage," *Energy*, Vol. 119, pp. 442–452 (2017).
9. Luo, X. J. and K. F. Fong, "Control optimization of combined cooling and power system with prime mover of solid oxide fuel cell-gas turbine for building application," *Energy Proc.*, Vol. 105, pp. 1883–1888 (2017).
10. Chandra Saikia, L. and S. Kant Sahu, "Automatic generation control of a combined cycle gas turbine plant with classical controllers using fire fly algorithm," *Elect. Power Energy Syst.*, Vol. 53, pp. 27–33 (2013).
11. Pan, Y., M. J. Er, T. Sun, B. Xu, and H. Yu, "Adaptive fuzzy PD control with stable H∞ tracking guarantee," *Neurocomputing*, Vol. 237, pp. 71–78 (2017).
12. Kurata, O., N. Iki, T. Matsunuma, et al., "Micro gas turbine cogeneration system with latent heat storage at the university: part III: temperature control schedule," *Appl. Therm. Eng.*, Vol. 70, pp. 705–715 (2014).
13. McLarty, D., J. Brouwer, and S. Samuelsen, "Fuel cell gas turbine hybrid system design part II: dynamics and control," *J. Power Sources*, Vol. 254, pp. 126–136 (2014).
14. Sorrentino, E. and P. Villafuerte, "Effect of the control of generators and turbines on the transient stability of a power system," *IEEE Latin Am. Trans.*, Vol. 14, No. 3, pp. 1227–1234 (2016).
15. Pan, Y., M. J. Er, R. Chen, and H. Yu, "Output feedback adaptive control without seeking spr condition," *Asian J. Control*, Vol. 17, No. 5, pp. 1620–1630 (2015).
16. Pan, Y., M. J. Er, Y. Liu, L. Pan, and H. Yu, "Composite learning fuzzy control of uncertain nonlinear systems," *Int. J. Fuzzy Syst.*, Vol. 18, No. 6, pp. 990–998 (2016).
17. Pan, Y., H. Yu, and M. J. Er, "Adaptive neural pd control with semiglobal asymptotic stabilization guarantee," *IEEE Trans. Neural Netw. Learn. Syst.*, Vol. 25, No. 12, pp. 2264–2274 (2014).
18. Bukala, J., K. Damaziak, H. Reza Karimi, and J. Malachowski, "Aero-elastic coupled numerical analysis of small wind turbine-generator modelling," *Wind Struct.*, Vol. 23, No. 6, pp. 577–594 (2016).
19. Tutiven, C., Y. Vidal, L. Acho, and J. Rodellar, "Hysteresis-based design of dynamic reference trayectories to avoid saturation in controlled wind turbines," *Asian J. Control*, Vol. 19, No. 2, pp. 438–449 (2017).
20. Aguilar-Ibañez, C., "Stabilization of the pvtol aircraft based on a sliding mode and a saturation function," *Int. J. Robust Nonlinear Control*, Vol. 27, pp. 843–859 (2017).
21. Li, S., H. Wang, Y. Tian, A. Aitouch, and J. Klein, "Direct power control of dfig wind turbine systems based on an intelligent proportional-integral sliding mode control," *ISA Trans.*, Vol. 64, pp. 431–439 (2016).
22. Senanayaka, J. S. L., H. Reza Karimi, and K. G. Robbersmyr, "Direct torque control of a small wind tur-

© 2017 Chinese Automatic Control Society and John Wiley & Sons Australia, Ltd

bine with a sliding-mode speed controller," *J. Phys.: Conf. Series*, Vol. 753, pp. 1–10 (2016).
23. Torchani, B., A. Sellami, and G. Garcia, "Variable speed wind turbine control by discrete-time sliding mode approach," *ISA Trans.*, Vol. 62, pp. 81–86 (2016).
24. Jafarnejadsani, H., J. Pieper, and J. Ehlers, "Adaptive control of a variable-speed variable-pitch wind turbine using radial-basis function neural network," *IEEE Trans. Control Syst. Technol.*, Vol. 21, No. 6, pp. 2264–2272 (2013).
25. Routray, S. K., R. K. Patnaik, and P. K. Dash, "Adaptive non-linear control of upfc for stability enhancement in a multimachine power system operating with a dfig based wind farm," *Asian J. Control*, Vol. 19, No. 5, pp. 1–20 (2017).
26. Aguilar-Ibañez, C., H. Sira-Ramirez, and J. A. Acosta, "Stability of Active Disturbance Rejection Control for Uncertain Systems: a Lyapunov Perspective," *Int. J. Robust Nonlinear Control* (2017). https://doi.org/10.1002/rnc.3812.
27. Ginter, V. J. and J. K. Pieper, "Robust gain scheduled control of a hydrokinetic turbine," *IEEE Trans. Control Syst. Technol.*, Vol. 19, No. 4, pp. 805–817 (2011).
28. Si, Y., H. Reza Karimi, and H. Gao, "Modelling and optimization of a passive structural control design for a spar-type floating wind turbine," *Eng. Struct.*, Vol. 69, pp. 168–182 (2014).
29. Bakka, T., H. Reza Karimi, and S. Christiansen, "Linear parameter-varying modelling and control of an offshore wind turbine with constrained information," *IET Contr. Theory Appl.*, Vol. 8, No. 1, pp. 22–29 (2014).
30. Jafarnejadsani, H. and J. Pieper, "Gain-scheduled optimal control of variable-speed-variable-pitch wind turbines," *IEEE Trans. Control Syst. Technol.*, Vol. 23, No. 1, pp. 372–379 (2015).
31. Teja Kandukuri, S., V. Khang Huynh, H. Reza Karimi, and K. Gunnar Robbersmyr, "Fault diagnostics for electrically operated pitch systems in offshore wind turbines," *J. Phys.: Conf. Series*, Vol. 753, pp. 1–14 (2016).
32. Toubakh, H. and M. Sayed-Mouchaweh, "Hybrid dynamic data-driven approach for drift-like fault detection in wind turbines," *Evolving Syst.*, Vol. 6, pp. 115–129 (2015).
33. Toubakh, H. and M. Sayed-Mouchaweh, "Hybrid dynamic classifier for drift-like fault diagnosis in a class of hybrid dynamic systems: Application to wind turbine converters," *Neurocomputing*, Vol. 171, pp. 1496–1516 (2016).
34. Pratama, M., S. G. Anavatti, M. J. Er, and E. Lughofer, "Pclass: An effective classifier for streaming examples," *IEEE Trans. Fuzzy Syst.*, Vol. 23, No. 2, pp. 369–386 (2015).
35. Pratama, M., J. Lu, E. Lughofer, G. Zhang, and M. J. Er, "An incremental learning of concept drifts using evolving type-2 recurrent fuzzy neural networks," *IEEE Trans. Fuzzy Syst.* (2016). https://doi.org/10.1109/TFUZZ.2016.2599855.

José de Jesús Rubio is a full time professor of the Sección de Estudios de Posgrado e Investigación, ESIME Azcapotzalco, Instituto Politécnico Nacional. He has published 105 papers in International Journals with 1000 citations.

Jesus Lopez is a Ph.D. student of the Sección de Estudios de Posgrado e Investigación, ESIME Azcapotzalco, Instituto Politécnico Nacional. He has published 3 papers in International Journals.

Jaime Pacheco is a full time professor of the Sección de Estudios de Posgrado e Investigación, ESIME Azcapotzalco, Instituto Politécnico Nacional. He has published 25 papers in international journals.

Rodrigo Encinas is a Ph.D. student of the Sección de Estudios de Posgrado e Investigación, ESIME Azcapotzalco, Instituto Politécnico Nacional. He has published 3 papers in International Journals.

© 2017 Chinese Automatic Control Society and John Wiley & Sons Australia, Ltd